Evidence for Hydraulic Vulnerability Segmentation and Lack of Xylem Refilling under Tension[1][OPEN]

Guillaume Charrier[2]*, José M. Torres-Ruiz, Eric Badel, Regis Burlett, Brendan Choat, Herve Cochard, Chloe E. L. Delmas, Jean-Christophe Domec, Steven Jansen, Andrew King, Nicolas Lenoir, Nicolas Martin-StPaul, Gregory Alan Gambetta, and Sylvain Delzon

Bordeaux Sciences Agro, Institut des Sciences de la Vigne et du Vin, Ecophysiologie et Génomique Fonctionnelle de la Vigne, Unité Mixte de Recherche 1287, F–33140 Villenave d'Ornon, France (G.C., G.A.G.); BIOGECO, INRA, Univ. Bordeaux, 33610 Cestas, France (G.C., J.M.T.-R., R.B., S.D.); PIAF, Institut National de la Recherche Agronomique, UCA, 63000 Clermont-Ferrand, France (E.B., H.C.); Hawkesbury Institute for the Environment, Western Sydney University, Richmond, New South Wales 2753, Australia (B.C.); Unité Mixte de Recherche SAVE, INRA, BSA, Univ. Bordeaux, 33882 Villenave d'Ornon, France (C.E.L.D.); Bordeaux Sciences Agro, Unité Mixte de Recherche 1391 ISPA, F–33882 Villenave d'Ornon, France (J.-C.D.); Nicholas School of the Environment, Duke University, Durham, North Carolina 27708 (J.-C.D.); Institute of Systematic Botany and Ecology, Ulm University, Ulm D–89081, Germany (S.J.); Synchrotron SOLEIL, L'Orme de Merisiers, Saint Aubin-BP48, 91192 Gif-sur-Yvette cedex, France (A.K.); Centre National de la Recherche Scientifique, Univ. Bordeaux, UMS 3626 Placamat F–33608 Pessac, France (N.L.); and INRA, UR629 Ecologie des Forêts Méditerranéennes, 84914 Avignon, France (N.M.-S.)

ORCID IDs: 0000-0003-1367-7056 (J.M.T.-R.); 0000-0003-2282-7554 (E.B.); 0000-0001-8289-5757 (R.B.); 0000-0002-2727-7072 (H.C.); 0000-0002-4476-5334 (S.J.); 0000-0001-7574-0108 (N.M.-S.); 0000-0002-8838-5050 (G.A.G.); 0000-0003-3442-1711 (S.D.).

The vascular system of grapevine (*Vitis* spp.) has been reported as being highly vulnerable, even though grapevine regularly experiences seasonal drought. Consequently, stomata would remain open below water potentials that would generate a high loss of stem hydraulic conductivity via xylem embolism. This situation would necessitate daily cycles of embolism repair to restore hydraulic function. However, a more parsimonious explanation is that some hydraulic techniques are prone to artifacts in species with long vessels, leading to the overestimation of vulnerability. The aim of this study was to provide an unbiased assessment of (1) the vulnerability to drought-induced embolism in perennial and annual organs and (2) the ability to refill embolized vessels in two *Vitis* species X-ray micro-computed tomography observations of intact plants indicated that both *Vitis vinifera* and *Vitis riparia* were relatively vulnerable, with the pressure inducing 50% loss of stem hydraulic conductivity = −1.7 and −1.3 MPa, respectively. In *V. vinifera*, both the stem and petiole had similar sigmoidal vulnerability curves but differed in pressure inducing 50% loss of hydraulic conductivity (−1.7 and −1 MPa for stem and petiole, respectively). Refilling was not observed as long as bulk xylem pressure remained negative (e.g. at the apical part of the plants; −0.11 ± 0.02 MPa) and change in percentage loss of conductivity was 0.02% ± 0.01%. However, positive xylem pressure was observed at the basal part of the plant (0.04 ± 0.01 MPa), leading to a recovery of conductance (change in percentage loss of conductivity = −0.24% ± 0.12%). Our findings provide evidence that grapevine is unable to repair embolized xylem vessels under negative pressure, but its hydraulic vulnerability segmentation provides significant protection of the perennial stem.

The plant hydraulic system is located at the interface between soil water and the atmosphere. Evaporative demand from the atmosphere generates a tension within a continuous xylem water column, pulling water from the soil, through roots, stems, petioles, and leaves (Dixon, 1896). Under drought conditions, the overall resistance to water flow through the soil-plant continuum increases. Increased resistance to water flow results from changes in the resistance at multiple specific locations along the flow pathway: in the soil, at the soil-root interface, and in the roots, the main plant axis (i.e. stems and branches), the petioles, and the leaves. Two primary mechanisms controlling the resistance are stomatal closure (leaf-to-air water flow) and the loss of xylem hydraulic conductivity (soil-to-leaf water flow; Cochard et al., 2002). Stomatal closure is closely related to decreasing plant water status (Brodribb and Holbrook, 2003) and is often considered to be a protective mechanism against the loss of xylem hydraulic conductivity (Tyree and Sperry, 1988; Jones and Sutherland, 1991). Loss of xylem hydraulic conductivity occurs when the water potential of xylem sap reaches levels negative enough to disrupt the metastability of the water column, potentially resulting in embolism.

Generally, high resistance to embolism is observed in species distributed in dry environments, whereas highly vulnerable species are distributed in wet environments (Maherali et al., 2004; Choat et al., 2012). Although grapevine (*Vitis* spp.) is widely cultivated, including in regions where it is frequently exposed to water deficit during the growing season (Lovisolo et al., 2010), recent studies have produced contrasting estimates of its resistance to embolism. Grapevine has been described as either vulnerable (Zufferey et al., 2011; Jacobsen and

Pratt, 2012) or relatively resistant (Choat et al., 2010; Brodersen et al., 2013). In *Vitis* spp., and *Vitis vinifera* especially, stomatal closure is typically observed for midday leaf water potentials less than −1.5 MPa (Schultz, 2003). Thus, according to some studies, significant losses in xylem hydraulic conductivity should be observed before stomatal closure ($\Psi_{50} > -1$ MPa; Jacobsen and Pratt, 2012; Jacobsen et al., 2015), implying that embolism would be commonplace.

The risk of hydraulic dysfunction is mitigated along the hydraulic pathway by hydraulic segmentation (i.e. more distal organs such as leaves and petioles will be at greater risk to embolism than more basal organs such as the trunk; Tyree and Zimmermann 2002; Choat et al., 2005). This could promote hydraulic safety in larger, perennial organs, which represent a greater investment of resources for the plant. Hydraulic segmentation may occur in two ways. During transpiration, the xylem pressure will always be more negative in more distal parts of the pathway (leaves and petioles). All else being equal, this translates to a greater probability of embolism in distal organs. However, organs also may differ in their vulnerability to embolism, compensating or exacerbating the effects of differences in xylem pressure along the pathway. If leaves or petioles were more vulnerable to embolism than branches and the trunk, then they would be far more likely to suffer embolism during periods of water stress. This would allow petioles, leaves (Nolf et al., 2015), or even young branches (Rood et al., 2000) to become embolized without significant impacts on the trunk and larger branches. In grapevine, petioles have been described as extremely sensitive to cavitation (Ψ_{50} of approximately −1 MPa; Zufferey et al., 2011). However, the hydraulic methods employed in those previous studies have been shown to be prone to artifacts (Wheeler et al., 2013; Torres-Ruiz et al., 2015), necessitating the use of a noninvasive assessment of drought-induced embolism.

High-resolution computed tomography (HRCT) produces three-dimensional images of xylem tissue in situ, allowing for a noninvasive assessment of embolism resistance. This technique has provided robust results in various plant species with contrasting xylem anatomy (Charra-Vaskou et al., 2012, 2016; Dalla-Salda et al., 2014; Torres-Ruiz et al., 2014; Cochard et al., 2015; Knipfer et al., 2015; Bouche et al., 2016). Synchrotron-based tomography facilities allow the visualization of intact plants, offering a noninvasive, in vivo estimation of the loss of hydraulic conductivity within the xylem (Choat et al., 2016). Moreover, the quality of the x-ray beam in the synchrotron facilities provides high resolution and signal-to-noise ratio, making image analysis simple and accurate.

If grapevine were as vulnerable to xylem embolism as suggested in some studies, refilling of embolized vessels would be expected to occur on a frequent (daily) basis in order to maintain hydraulic continuity (Sperry et al., 1994; Cochard et al., 2001; Hacke and Sperry, 2003; Charrier et al., 2013). Various refilling mechanisms have been proposed to date, including positive root/stem pressure and refilling while the xylem is under negative pressure via water droplet growth (Salleo et al., 1996; Brodersen et al., 2010; Knipfer et al., 2016). Positive pressure in the xylem sap can be related to mineral nutrition and soil temperature in autumn or spring (Ewers et al., 2001) and to soluble carbohydrate transport into the vessel lumen during winter (Améglio et al., 2001; Charrier et al., 2013). Refilling under negative pressure is based on the hypothesis that embolized vessels are isolated from surrounding functional vessels, permitting positive pressures to develop and the embolism to dissolve (Salleo et al., 1996; Tyree et al., 1999). This process has been related to the chemistry of conduit walls (Holbrook and Zwieniecki, 1999), the geometry of interconduit bordered pits (Zwieniecki and Holbrook, 2000), and phloem unloading (Nardini et al., 2011). While refilling via positive pressure has been described frequently (Sperry et al., 1987, 1994; Hacke and Sauter 1996; Cochard et al., 2001; Améglio et al., 2004; Cobb et al., 2007), refilling under negative pressure remains controversial (Cochard et al., 2013, 2015). In grapevine particularly, imaging techniques have provided evidence of refilling in embolized vessels (Brodersen et al., 2010), but uncertainties remain regarding the xylem water potential measurement at the position of the scan.

The goal of this study was to provide a noninvasive assessment of (1) the vulnerability to drought-induced embolism in two widespread grapevine species in perennial (*V. vinifera* and *Vitis riparia*) and annual (*V. vinifera*) organs and (2) the ability to refill embolized vessels under positive or negative pressure (*V. vinifera*). This approach would indicate whether embolism formation

[1] This work was supported by the Cluster of Excellence COTE (grant no. ANR–10–LABX–45, within Water Stress and Vivaldi projects) and the AgreenSkills Fellowship program, which received funding from the European Union's Seventh Framework Program (grant no. FP7 26719, AgreenSkills contract no. 688), by the program Investments for the Future (grant no. ANR–10–EQPX–16, XYLOFOREST) from the French National Agency for Research, by the Australian Research Council (Future Fellowship no. FT130101115 to B.C.), and by travel funding to B.C. from the International Synchrotron Access Program managed by the Australian Synchrotron.

[2] Present address: Unité Mixte de Recherche 1202, Biodiversité Gènes en Communautés, Institut National de la Recherche Agronomique/Université Bordeaux, Bâtiment B2, Allée G. St Hilaire, CS 50023, 33615 Pessac cedex, France.

* Address correspondence to guillaume.charrier@bordeaux.inra.fr.

The author responsible for distribution of materials integral to the findings presented in this article in accordance with the policy described in the Instructions for Authors (www.plantphysiol.org) is: Guillaume Charrier (guillaume.charrier@bordeaux.inra.fr).

G.A.G., G.C., S.D., and C.E.L.D. conceived the original screening and research plans; G.C., E.B., A.K., N.L., R.B., J.M.T.-R., H.C., N.M.-S., S.J., B.C., and S.D. performed the HRCT scans; G.C. and J.M.T.-R. performed leaf hydraulics experiments; G.C. and J.-C.D. performed gas-exchange experiments; C.E.L.D. provided plant materials; G.C., G.A.G., and S.D. analyzed the data and wrote the article with contributions of all the authors.

[OPEN] Articles can be viewed without a subscription.

www.plantphysiol.org/cgi/doi/10.1104/pp.16.01079

and repair are likely to occur on a daily basis and/or if hydraulic segmentation could protect perennial organs from drought stress. Stems and petioles from intact *V. vinifera* 'Cabernet Sauvignon' and *V. riparia* plants were scanned using Synchrotron-based HRCT, characterizing their vulnerability to embolism and quantifying their ability to refill at different positions along the plant axis (base and apex) in relation to bulk xylem pressure. These data were integrated with other noninvasive techniques assessing leaf hydraulics and transpiration.

RESULTS

HRCT Imaging and Embolism Vulnerability in *V. vinifera* and *V. riparia*

Embolism in stems (*V. vinifera* and *V. riparia*) and petioles (*V. vinifera*) was characterized by direct observation provided by HRCT images. Two-dimensional, transverse slices of xylem were extracted from a three-dimensional volume for image analysis. Typical cross sections are presented in Figure 1 for *V. vinifera*. Embolized (i.e. air-filled) vessels appear as black spots (highlighted red in insets). Well-hydrated plants (stem water potential [Ψ_{Stem}] > -0.5 MPa) exhibited none or very few air-filled vessels in stems and petioles (Fig. 1, A and D). For both organs, the percentage loss of conductivity (PLC) measured was lower than 5%. At further dehydration (approximately -1.1 MPa), only a few vessels became air filled in stems generating 9% loss of hydraulic conductance (Fig. 1B), whereas half of the vessels were already embolized in petioles (PLC = 46.2%; Fig. 1E). A more negative water potential ($\Psi_{Stem} = -1.7$ MPa) induced a considerable increase in the number of air-filled vessels in both stems and petioles, PLC reaching 50.5% and 96.5%, respectively (Fig. 1, C and F).

HRCT imaging was used to establish stem vulnerability curves (i.e. variation in PLC as a function of xylem pressure). In *V. vinifera*, vulnerability curves of both organs exhibited a similar sigmoid shape, with the air-entry point (Ψ_e) observed at -1.22 and -0.26 MPa in stems and petioles, respectively (Fig. 2; Table I). Water potential inducing 50% loss of hydraulic conductance differed between stems ($\Psi_{50Stem} = -1.73$ MPa) and petioles ($\Psi_{50Petiole} = -0.98$ MPa). Thus, when the water potential reached stem Ψ_e, petioles had already lost 66% of their conductivity. Significant differences were observed between *Vitis* spp. ($P = 0.002$; Fig. 3), with *V. riparia* being more vulnerable than *V. vinifera* ($\Psi_e = -0.70$ versus -1.22 MPa and $\Psi_{50Stem} = -1.29$ versus -1.73 MPa for *V. riparia* and *V. vinifera*, respectively).

Integration with Leaf Hydraulic Conductance and Gas Exchange in *V. vinifera*

Changes in leaf hydraulic conductance (denoted as K_{Leaf}, but including part of the petiole) and transpiration were assessed, and the data were integrated with those obtained from the HRCT analyses above. Loss of K_{Leaf} exhibited a similar pattern to loss of hydraulic conductance in petioles: $\Psi_{50Petiole} = -0.98$ MPa and $\Psi_{50Leaf} = -1.08$ MPa (Table I), although with differences in the sensitivity ($69\% < slp < 129\%$ MPa^{-1}), where *slp* is the derivative at the inflection point. Apparent K_{leaf} (K_{Leaf_Ap}) was shifted compared with K_{Leaf} (similar sensitivity, 134% MPa^{-1}; and higher Ψ_{50Leaf_Ap}, -0.46 MPa). Parameters of all vulnerability curves were significantly different from 0 ($P < 0.001$; Table I).

Considering the stem-to-leaf gradient in water potential measured during the gas-exchange experiment (i.e. when stomata remained open and water potential gradient was maintained; $\Psi_{Stem} = 0.866 \times \Psi_{Leaf} + 0.083$;

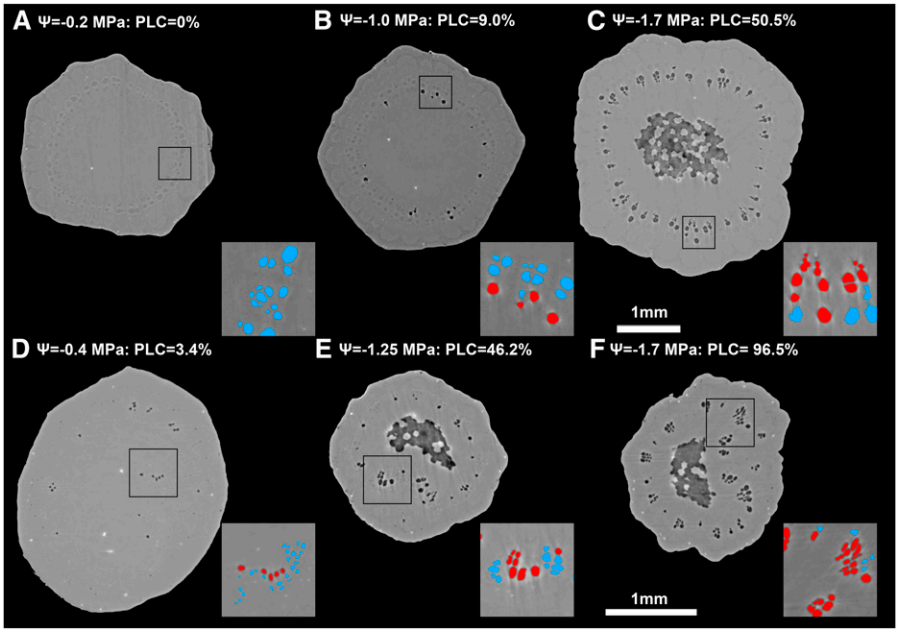

Figure 1. Transverse HRCT images of intact *V. vinifera* 'Cabernet Sauvignon' plants at different water potentials: stems (A–C) and petioles (D–F). Insets represent 0.25-mm^2 areas. Functional (gray) and air-filled (black) xylem vessels are represented in blue and red in the insets, respectively. The theoretical loss of hydraulic conductivity for each image is indicated as PLC (%). Bars = 1 mm.

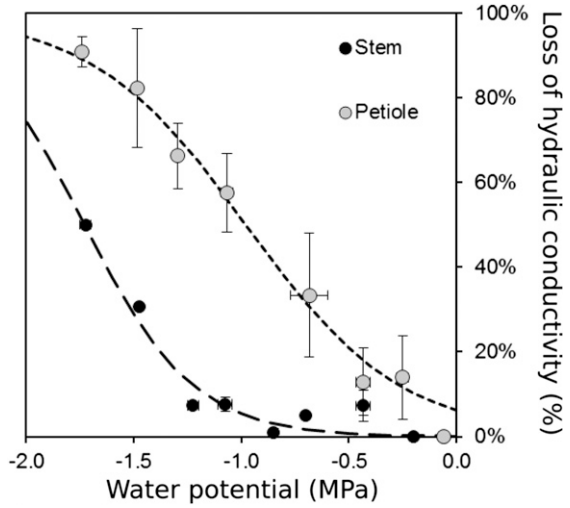

Figure 2. Percentage loss of hydraulic conductivity (%) versus xylem water potential (MPa) calculated from HRCT images in *V. vinifera* stems (black circles) and petioles (gray circles). Dashed lines represent the sigmoid fits of the data. Symbols and bars represent means and SE from 0.2-MPa classes (n = 1–7 replicates per circle).

r^2 = 0.870), loss of hydraulic function across stems, petioles, and leaves was calculated depending on Ψ_{Leaf} (Fig. 4). The petiole and leaf were closely coordinated, with 50% loss of function at approximately −1 MPa, whereas the stem remained almost nonembolized (PLC = 2.5%) at this water potential and transpiration was reduced (5.4%). At lower water potentials, almost complete hydraulic dysfunction in petioles ($PLC_{Petiole}$ = 88% at Ψ = −1.7 MPa) was observed, and the stem exhibited significant embolism (PLC_{Stem} = 32.2%). The margin between Ψ_{50Stem} and either $\Psi_{50Petiole}$ or Ψ_{50Leaf} was relatively narrow (0.65–0.75 MPa). However, taking the gradient in Ψ from stem to leaf into account, the effective safety margin was slightly greater (0.8–0.9 MPa). Under well-watered conditions, with high vapor pressure deficit (approximately 2,500 Pa), leaf and stem water potentials reached −0.62 ± 0.03 MPa and −0.39 ± 0.03 MPa (mean ± SE; n = 36) for leaves and stems, respectively. Under the normal operating range of water potential, therefore, the amount of PLC in the stem and petiole would be low (0% and 17%, respectively), while transpiration would be limited (K_{ap} = 42%).

Xylem Refilling in *V. vinifera*

Rewatered plants were scanned either in the basal part (1 cm above the grafting) or in the distal part (approximately 1 m above soil). In the basal part, significant changes in the amount of air-filled vessels were observed over a 24-h period after the plant was rewatered. Most vessels were dark gray (i.e. air filled) before rewatering (PLC = 86.8%; Fig. 5D). After 7.5 h, evidence of xylem refilling and an increase in the number of functional vessels were observed (Fig. 5E), even though PLC was barely affected (PLC = 81.2%). After 15.5 h, many additional vessels had refilled, decreasing the PLC to 57.4% (Fig. 5F). In contrast, in the upper part of rewatered plants, even after more than 48 h of rewatering, there was no significant change in PLC (Fig. 5, A–C), even though most living cells remained alive (Supplemental Fig. S1). Refilling was not observed at the apex (change in PLC [ΔPLC] = 0.02% ± 0.01%), regardless of the initial levels of embolism (13.7% < PLC < 92.4%).

Figure 6 depicts the changes in basal and apical portions of the same plant, where xylem refilling was observed at the base (ΔPLC = −15.5%) and, at the same moment, no significant change in PLC was observed in the upper part (ΔPLC = +5.7%). Pressure transducers indicated that bulk xylem pressure was positive at the base (Ψ_{Stem} = +0.023 MPa) and negative at the apex (Ψ_{Stem} = −0.015 MPa). Although stem water potential quickly increased after rewatering, it did not completely equilibrate along the whole stem even after more than 80 h (Supplemental Fig. S2). Negative pressure was measured at the apex (Ψ = −0.013MPa), whereas it was positive at the base of the same plant (Ψ_{Stem} = +0.033 MPa). Although not all plants exhibited individual vessels being refilled with sap or positive pressure, significant changes in theoretical hydraulic conductance were observed only when xylem pressures were positive (Fig. 7A). Thus, differences in water potential (P = 0.011) and PLC (P = 0.006) were observed depending on the distance from the soil among the five replicates (Fig. 7B).

Table I. *Details of the fits of different experimental data with a sigmoid function in V. vinifera*

Different techniques were used according to the studied organ: HRCT image analysis in stems and petioles, measurement of rehydration kinetics at the leaf level, and measurement of transpiration loss depending on the water potential gradient from leaf to root. Degrees of freedom (Df), residual sum of squares (SSres), and pseudo-r^2 are given. Values and significance of the two parameters (slope and Ψ_{50}) are indicated (***, $P < 0.0001$), and Ψ_e was calculated from these latter parameters.

Organ	Technique	Df	SSres	Pseudo-r^2	Slope	Ψ_{50}	Ψ_e
					% MPa^{-1}	MPa	
Stem	HRCT	15	0.158	0.905	98.4***	−1.729***	−1.221
Petiole	HRCT	25	0.753	0.737	69.3***	−0.980***	−0.259
Leaf	Rehydration	32	0.207	0.948	129.0***	−1.084***	−0.696
Leaf	Transpiration	74	2.171	0.596	133.6***	−0.456***	−0.830

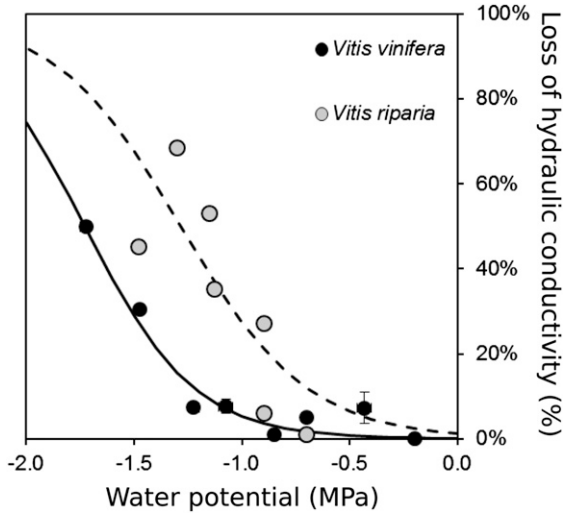

Figure 3. Percentage loss of hydraulic conductivity (%) versus xylem water potential (MPa) calculated from HRCT images in stems of *V. vinifera* (black circles) and *V. riparia* (gray circles). Lines represent the sigmoid fits of the data (solid and dashed lines for *V. vinifera* and *V. riparia*, respectively). Symbols and bars represent means and SE from 0.2-MPa classes in *V. vinifera* (n = 1–7 replicates per circle) and *V. riparia* (n = 1 replicate per circle).

DISCUSSION

Despite the fact that *V. vinifera* can be adapted to environments experiencing seasonal drought, studies differ in estimates of its hydraulic vulnerability and its classification as drought sensitive (Wheeler et al., 2005; Jacobsen and Pratt, 2012) or drought resistant (Choat et al., 2010; Brodersen et al., 2013). Discrepancies among studies most likely lie in methodological issues, especially considering that *V. vinifera* is a long-vesseled species (Cochard et al., 2013; Rockwell et al., 2014; Zhang and Holbrook, 2014). Here, to our knowledge for the first time, a noninvasive estimation of complete vulnerability curves was obtained using direct observations on intact *Vitis* spp. by HRCT. Our results demonstrate that *V. vinifera* stems are more resistant to xylem embolism than estimated previously by centrifugation techniques and can sustain water potential lower than −1 MPa (Ψ_{50Stem} = −1.7 MPa). In contrast, *V. riparia* originates from riparian habitats and exhibited higher drought sensitivity (Ψ_{50Stem} = 1.3 MPa). Our findings also show that petioles are more vulnerable to embolism than stems, providing evidence for hydraulic vulnerability segmentation in grapevine. Xylem conduit refilling was observed in the basal part of the plant, where positive bulk pressure was recorded (Figs. 5, D–F, and 6), but not in the apical part, where bulk pressure remained negative under experimental conditions (Figs. 5, A–C, and 6).

In view of the current debate on drought resistance of long-vesseled species (Sperry et al., 2012; Cochard and Delzon, 2013; Sperry, 2013; Cochard et al., 2015; Hacke et al., 2015), vulnerability curves imply either that embolism occurs almost immediately under negative water potentials of the xylem sap (exponential vulnerability curves) or that embolism does not take place until a threshold at a more negative water potential is reached (sigmoidal vulnerability curves). According to Figure 1, no embolism was observed at high xylem water potentials ($\Psi > -1$ MPa) in stems of intact *V. vinifera* plants, suggesting that all vessels can support some level of negative pressure. In stems, the number of embolized vessels increased only once the pressure reached values lower than −1.5 MPa, which is consistent with results observed using magnetic resonance imaging (MRI; Choat et al., 2010) and HRCT (Knipfer et al., 2015). Nonfunctional vessels (i.e. those that remained full of sap on our final-cut images) represented approximately 5% of the theoretical conductance and were not included in our vulnerability curve analyses.

The high image resolution (approximately 3 μm per voxel) provided by HRCT allowed the computation of a theoretical conductivity according to the diameters of individual vessels via the Hagen-Poiseuille equation (Figs. 2 and 3). Therefore, the theoretical loss of conductance could be quantified at various xylem water potentials (Brodersen et al., 2013), whereas previous studies qualitatively assessed PLC from the number of air-filled versus sap-filled vessels. Combined with a high number of specimens at a wide range of water potentials, these results provide, to our knowledge for the first time, a complete vulnerability curve for intact stems (Ψ_{50Stem} = −1.73 MPa) and petioles ($\Psi_{50Petiole}$ = −0.98 MPa) of *V. vinifera*. The vulnerability curves obtained are in agreement with the level of drought-induced embolism resistance observed for

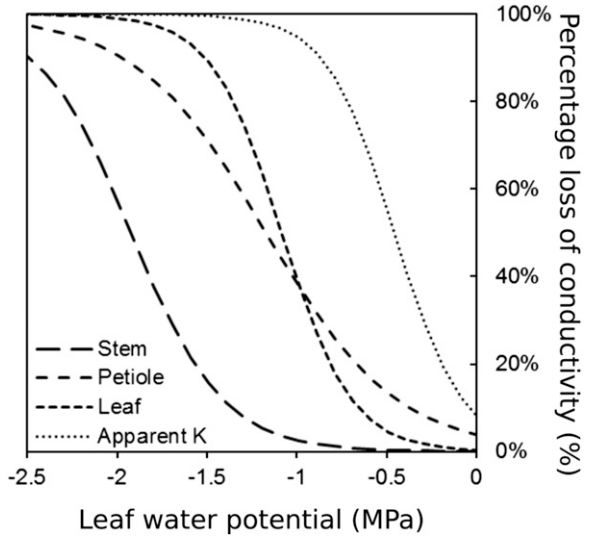

Figure 4. Percentage loss of hydraulic conductivity (%) in *V. vinifera* stems (solid line; HRCT images), petioles (long-dashed line; HRCT images), leaves (short-dashed line; rehydration kinetic method), and apparent leaf conductance (dotted line; calculated from gas-exchange measurements) depending on leaf water potential (MPa).

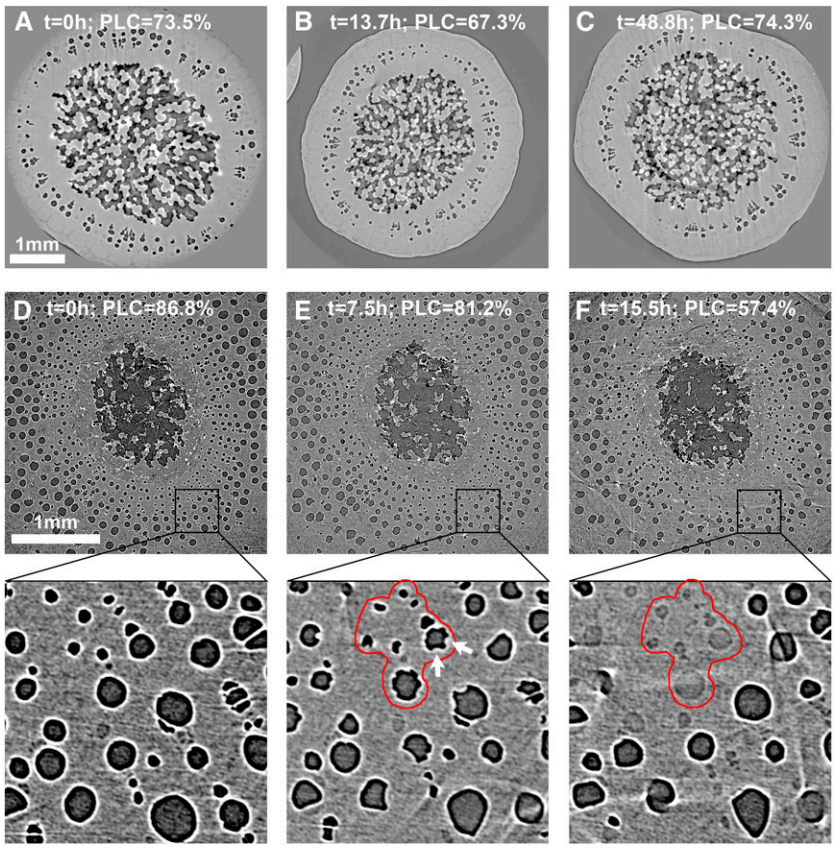

Figure 5. Cross sections of *V. vinifera* stems at two different height levels, the upper, distal part (A–C) and the lower, proximal part above the graft (D–F), after rewatering drought-stressed plants. Time relative to rewatering (t = 0 h; i.e. the rewatering time) and the theoretical losses of hydraulic conductance (PLC; %) are indicated. Bars = 1 mm.

grapevine in studies using noninvasive techniques, such as synchrotron-based HRCT (Brodersen et al., 2013), acoustic emission analysis (Vergeynst et al., 2015), and MRI (Choat et al., 2010). Although the source and signal interpretation qualitatively differ across noninvasive techniques, numerous studies combining these techniques in various species measured similar levels of embolism resistance (Choat et al., 2010, 2016; Charra-Vaskou et al., 2012, 2016; Charrier et al., 2014; Ponomarenko et al., 2014; Torres-Ruiz et al., 2014; Vergeynst et al., 2015). However, the Ψ_{50} values observed in this study are slightly less negative than those reported previously with noninvasive methods (−1.7 versus approximately −2 MPa). This may be due to differences in plant material. Ontogenic developmental stages of the plant might explain this discrepancy, where the development of secondary xylem during the season would increase embolism resistance in grapevine (Choat et al., 2010). Our results demonstrate genotypic differences in stem vulnerability curves between *Vitis* spp. (*V. vinifera* versus. *V. riparia*; Fig. 3) and are consistent with the higher drought sensitivity of *V. riparia* compared with *Vitis arizonica* and *Vitis champinii* (Knipfer et al., 2015).

Petioles were more vulnerable to embolism than stems in *V. vinifera* 'Cabernet Sauvignon' (Figs. 1 and 2). Only a few studies have reported petiole vulnerability curves for grapevine. Similar behavior is reported in other *V. vinifera* cultivars using a flowmeter (Zufferey et al., 2011), a pressure sleeve (Tombesi et al., 2014), or MRI (Hochberg et al., 2016). Loss of conductance in petioles (HRCT based) and leaves (rehydration kinetic method) as measured with different techniques are remarkably similar (Fig. 4), even though computations of hydraulic conductance from HRCT image data are only theoretical. Considering an inaccuracy of two voxels per vessel, average vessel diameters exhibited approximately 11% and 19% deviation in stem and petiole, respectively. However, PLC values were affected only slightly (±09% in stem and petiole). HRCT-based images indicated that xylem embolism limits conductance in petioles. However, the minimum water potential experienced by the petiole might have been lower than that measured despite bagging the petiole for 3 h before scanning it. This would have led to slightly overestimated vulnerability curves and would require additional observations using, for example, a small-sized psychrometer to monitor the petiole water potential during dehydration. In leaves, xylem embolism and extraxylary (e.g. symplasmic) pathways both seem to contribute to the reduction of K_{Leaf} (Kim and Steudle, 2007; Scoffoni et al., 2014; Bouche et al., 2016). These results question the validity of stem water potential measurement using bagged leaves for high levels of stress (as presented in Fig. 6; i.e. when the leaf is hydraulically disconnected from the stem). Although embolism in petioles could represent a hydraulic fuse at the leaf level, under well-watered conditions, reduced

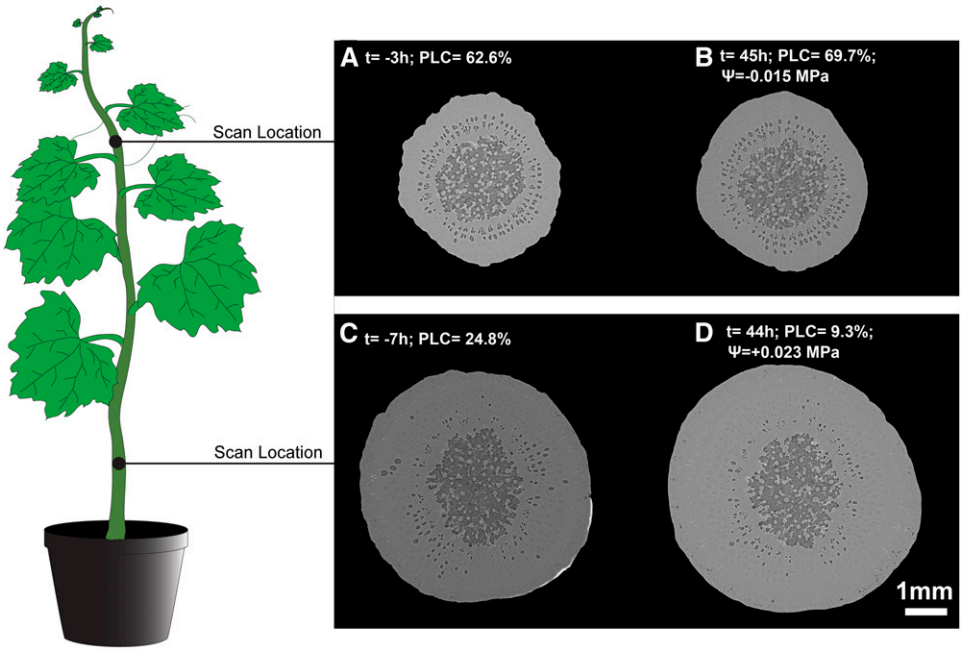

Figure 6. Cross sections at two different height levels, the upper, distal part (A and B) and the lower, proximal part above the graft (C and D), of the same *V. vinifera* plant before and after rewatering. Time relative to rewatering (t = 0 h; i.e. the rewatering time), theoretical losses of hydraulic conductance (PLC), and water potential (MPa) measured using a pressure chamber on a bagged leaf (Ψ_{leaf}), a stem psychrometer (Ψ_{stem}), and pressure probes are indicated. The discrepancy between Ψ_{leaf} and Ψ_{stem} probably originates from the disconnection between the stem and leaf hydraulic pathways (according to Fig. 4, when PLC_{apex} = 63%, Ψ_{leaf} = approximately −2 MPa, and $PLC_{petiole}$ = approximately 100%). Bar = 1 mm.

transpiration (approximately 40%) substantially limits petiole embolism to less than 20%. In addition, the relatively young plant material used in this study (1–2 months old) is relatively vulnerable (Choat et al., 2010), but typically, it would not experience substantial drought in springtime.

A gradient in water potential along the entire plant might prevent embolism from propagating from distal to proximal parts without considerable difference in an organ's embolism vulnerability per se (Fig. 6; Bouche et al., 2016). However, major anatomical differences in secondary growth, pit anatomy, and cell wall composition also could explain the higher embolism resistance of lignified organs, presenting fewer nucleation points and lower primary xylem-secondary xylem ratio (Choat et al., 2005). Resistance to embolism is indeed tightly linked to xylem anatomy at the interspecific level (Lens et al., 2011): air bubbles nucleating onto cell walls and propagate through pores of pit membrane (Jansen et al., 2009; Schenk et al., 2015). Through the gradient in water potential and hydraulic vulnerability segmentation, leaves and petioles isolate perennial parts of the plant from more negative water potentials and hydraulic failure under water deficit in grapevine (as demonstrated in this study) and some tropical tree species (Nolf et al., 2015).

This study provides new lines of evidence regarding the potential artifacts that lead to vulnerability curves with an exponential shape. The ratio between vessel and sample length impairs hydraulic measurements in long-vesseled species (Ennajeh et al., 2011; Martin-StPaul et al., 2014; Torres-Ruiz et al., 2014; Choat et al., 2016), although this is disputed by other studies (Sperry et al., 2012; Pratt et al., 2015). Furthermore, the exponential-shaped vulnerability curves imply that a grapevine stem would be 50% embolized before its leaf and stomatal conductance decrease, which seems unlikely (Nardini and Salleo, 2000). Moreover, investing carbon into structures (i.e. conduit walls) that would lose their function so readily seems unlikely, especially considering the functional importance of carbon in plant physiology (Mencuccini, 2003; McDowell, 2011; Sala et al., 2012; Hartmann et al., 2013; Charrier et al., 2015; Hartmann, 2015). Finally, the minimal water potential experienced by a plant on a seasonal basis is generally less negative than its Ψ_{50} value (Choat et al., 2012).

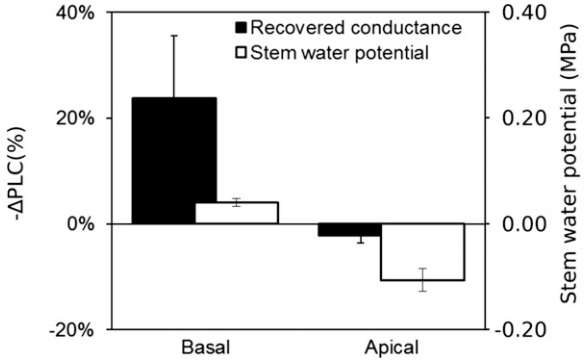

Figure 7. Mean changes in theoretical hydraulic conductance (−ΔPLC; %) and xylem water potential (MPa) for basal and apical scan positions in rewatered stems of *V. vinifera*. PLC and xylem water potential were significantly different across the apical and basal positions based on a Kruskal-Wallis test (n = 5; P = 0.006 and 0.011 for PLC and water potential, respectively).

This study does not support the high vulnerability of grapevine stems (Jacobsen et al., 2015). In this study, drought-stressed *V. vinifera* plants (10%–90% stem PLC) were able to refill embolized vessels at the stem bases but not at the upper, distal stem portions (Figs. 5 and 6). When observed, embolism refilling was always associated with positive root pressure (Fig. 7), consistent with the results of Knipfer et al. (2015). In the upper part, the xylem sap remained at negative pressure (Supplemental Fig. S2) and showed no refilling, even though vessel-associated cells remained alive (Supplemental Fig. S1). Root pressure has been credited as a strategy to recover from winter embolism (Ewers et al., 2001) and has been observed in various angiosperm dicot species, such as *Alnus* spp. (Sperry et al., 1994), *Betula* spp. (Sperry, 1988), *Juglans* spp. (Améglio et al., 2002; Charrier et al., 2013), *Vitis* spp. (Hales, 1727; Sperry et al., 1987), and some tropical and temperate vines and lianas (Ewers et al., 1997; Cobb et al., 2007). These studies suggest that particular species are able to actively refill their vessels by the generation of positive pressure in the early spring. In both this and previous studies, HRCT-based observations of xylem refilling in grapevine reveal water droplets clinging on vessel walls, which then increase in volume toward the center of the conduit lumen (Brodersen et al., 2013; Knipfer et al., 2015; Fig. 5). This may suggest that apoplastic sap is pressurized before invading the conduits' lumen. Recently, Knipfer et al. (2016) reported xylem refilling in the absence of a root system (i.e. in 3- to 5-cm-long excised stem segments connected to a 2-cm tube filled with a solution at 0.2 kPa [corresponding to 2-cm column height]). However, excised segments no longer exhibited tension or pressure and showed slight hydrostatic pressure when connecting the sample at both ends, which, combined with capillary forces, might have been sufficient to observe xylem refilling. In this study, even xylem positive pressure did not lead successfully to xylem refilling in all cases. Xylem pressures of 0.02 to 0.05 MPa magnitude were observed, which should correspond to a 2- to 5-m-high water column, while the apical portion remained at a slightly negative potential (-0.02 to -0.1 MPa) without refilling observed at the apex (Fig. 7). Xylem pressure may have been dissipated along the plant stems and/or gas did not dissolve into xylem sap, delaying the occurrence of positive pressure at higher parts. Although xylem refilling was not observed at the apex during our experiment, it may have occurred after a longer period. However, the occurrence of negative water potential after more than 3 d without active transpiration suggests that this phenomenon is not routine for *V. vinifera*. It is important to consider that only bulk xylem pressures were assessed in this study. There is a possibility that pressure gradients are not homogenous across a portion of the stem or even between vessels that lie in close proximity to each other. Currently, experimental approaches do not exist for assessing in situ pressures at this scale, but this difficulty needs to be acknowledged. Given that refilling is a phenomenon occurring at the level of an individual vessel, one would expect that it would be the local pressure gradient environment that would dictate whether refilling would occur, and not necessarily the bulk level property or the living cells' activity.

Previous observations of refilling under negative pressure may have resulted from artifacts such as those documented by Wheeler et al. (2013). Cutting stems under water when sap is under negative pressure may induce the artificial formation of air bubbles, leading to an overestimation of embolism vulnerability (Torres-Ruiz et al., 2015; Ogasa et al., 2016; Umebayashi et al., 2016). Therefore, normal diurnal fluctuation in xylem tension could produce artifactual PLC fluctuations in stems (Torres-Ruiz et al., 2015) or petioles (Zufferey et al., 2011). Equally, variation in tension along the plant axis could cause misleading interpretations of refilling under negative pressure if the leaves sampled for measuring stem water potential are not directly adjacent to the part of the stem being scanned and/or if leaves experienced levels of stress great enough to result in their hydraulic disconnection from the parent plant. Thus, we observed negative leaf water potential, although bulk xylem pressure was positive at the base (Fig. 6). This point should be of particular concern in light of the high vulnerability of grapevine petioles characterized in this and other studies. Water potential measurements, therefore, would have to be performed on downward leaves located as close as possible to the position of the HRCT area scanned (but only for a moderate level of stress). Alternative methods could include cutting stem segments after equilibration to atmospheric pressure or the use of stem psychrometers.

CONCLUSION

Stems of *V. vinifera* are more resistant to drought stress than those of *V. riparia* and are not able to refill under negative bulk xylem pressure. The hydraulic segmentation generated from stem to leaf is reinforced by vulnerability segmentation between perennial and annual parts, which prevents perennial parts from experiencing more severe losses in hydraulic function. The insights obtained here about the drought response of *Vitis* spp. highlight the limitations of current methods to assess in situ xylem sap water potential. These results will help assess the drought resistance of different grapevine genotypes and to manage irrigation in the field, and also should be of significant interest for other economically important long-vesseled plants (e.g. *Quercus* spp., *Olea* spp., and *Eucalyptus* spp.).

MATERIALS AND METHODS

Plant Material

Two widespread grapevine species were measured: *Vitis vinifera*, which is cultivated for grape production, and *Vitis riparia*, which is commonly used as a rootstock. The domesticated grapevine species *V. vinifera* originates from the Caucasian area (Zecca et al., 2012) and has been cultivated worldwide. This species was compared with *V. riparia*, a native American grape distributed in North America, which is known to be much more drought sensitive than

V. vinifera (Carbonneau, 1985). One-year-old potted plants from *V. vinifera* 'Cabernet Sauvignon' and *V. riparia* 'Gloire de Montpellier', both grafted on *V. riparia* 'Gloire de Montpellier' were grown in 7.5-L pots filled with commercial potting soil for 2 months until they reached approximately 1-m height and 1-cm basal stem diameter (five to 10 leaves). Different sets of plants ($n = 5$ to 10 plants per pool) were used for HRCT scans, K_{Leaf}, and gas-exchange measurements (see below).

In the HRCT pool, 10 *V. vinifera* and 10 *V. riparia* plants were exposed to different levels of water stress for 1 to 3 weeks to cover a wide range of water potentials. In 2015, the plants were scanned at approximately 1-m height two to three times during the 4-d HRCT observations (mid April 2015). Among this pool, three *V. vinifera* plants were rewatered after scanning until the soil was water saturated to measure their ability to recover from different levels of initial embolism ($50\% < PLC < 90\%$) in the upper part. Rewatered plants were stored in shaded conditions to prevent active transpiration (Holbrook et al., 2001) and scanned every 6 h for up to 48 h, while stem water potential was measured regularly (see details below). An additional rewatering experiment was performed in May 2016, on five additional plants of the same age and morphology as in 2015, focusing on the difference between apex and base (right above the rootstock). The K_{Leaf} measurements were carried out 2 months later (June 2015) on eight well-hydrated plants of *V. vinifera*, which were uprooted prior to measurements to allow their progressive dehydration within a daily course. In the gas-exchange pool, eight *V. vinifera* plants were exposed to different levels of water stress, but of lower intensity than the HRCT plants (predawn water potentials greater than −1.2 MPa).

HRCT

Synchrotron-based computed microtomography was used to visualize air-filled and sap-filled vessels in the main stem and petiole of *V. vinifera* 'Cabernet Sauvignon' and the main stem of *V. riparia*. In April 2015, plants were brought to the HRCT beamline (PSICHE) at the SOLEIL synchrotron facility. This beamline has a large, empty rotary stage, which allowed us to scan plants at different heights (e.g. basal and upper portions). Three hours before each scan, one leaf, located 10 mm above the scanned area, was wrapped in a plastic bag and covered with aluminum foil in order to provide accurate Ψ_{Stem} values. The water potential was then measured right before the scan with a Scholander pressure chamber (Precis 2000). At the height of the scan, one leaf was carefully attached to the stem using a piece of tape. The main stem and petiole were scanned simultaneously using a high-flux (3×10^{11} photons mm^{-2}) 25-keV monochromatic x-ray beam. The projections were recorded with a Hamamatsu Orca Flash sCMOS camera equipped with a 250-μm-thick LuAG scintillator. The complete tomographic scan included 1,500 projections, 50 ms each, for a 180° rotation. Thus, samples were exposed for 75 s to the x-ray beam. Tomographic reconstructions were performed using PyHST2 software (Mirone et al., 2014) using the Paganin method (Paganin, 2002), resulting in $1{,}536^3$ 32-bit volumic images. The final spatial resolution was 3^3 μm^3 per voxel. Complementary measurements to visualize embolized conduits in grapevine petioles and refilling at the stem base were undertaken at the Diamond Light Source and Swiss Light Source synchrotron facilities, where similar plant material and the same experimental setup were used. For details of the I12 beamline (Diamond Light Source) and the TOMCAT X02DA beamline (Swiss Light Source), see Bouche et al. (2016) and Choat et al. (2016), respectively.

Measurement of Xylem Pressure/Tension

During rewatering experiments, xylem water potential was measured using three different setups (Supplemental Fig. S2). Two were dedicated to measure xylem negative pressure: Scholander pressure chamber (described above) and psychrometers (PSY-1; ICT International). In the 2015 experiment, xylem water potential was measured only using the Scholander pressure chamber. In 2016, stem psychrometers were mounted on the stems of two different plants, 10 cm above grafting, before rewatering. A 5-cm-long portion of the stem was wrapped in Parafilm (Alcan) to ensure psychrometer sealing at 5 to 10 cm below the scanning area. About 2 cm^2 of bark (and Parafilm) was removed, and a psychrometer was attached with clamps. The third setup was dedicated to measure positive xylem pressure. When a clear decrease in the amount of embolized conduits was observed at the base, the apex of the plant was cut and immediately connected to a pressure transducer probe (26PCFFA6D; Honeywell) using an adapter tube filled with deionized and degassed water (Thitithanakul et al., 2012). Data were recorded on a CR1000 logger (Campbell) at a time interval of 30 s. Once the signal stabilized (approximately 15 min), the base was cut and connected to the pressure transducer following the same procedure.

Image Analysis and Vulnerability Curves

On transverse cross sections taken from the center of the scanned volume, the diameter and area of each individual air- and sap-filled vessel (embolized and functional, respectively) were measured in stems and/or petioles of each species using ImageJ software (http://rsb.info.nih.gov/ij). Air-filled vessels were highly contrasted with surrounding tissues. Thus, a binary image was generated and vessels were extracted according to their dimensions, discarding particles lower than 10 μm^2 (approximately four pixels).

After synchrotron experiments, all stems and petiole samples were wrapped in moist paper and plastic bags and brought to the PIAF-INRA laboratory. Samples were cut 2 mm above the previously scanned area and scanned again using HRCT (Nanotom 180 XS; GE) as described by Cochard et al. (2015). Vessels where sap was under negative pressure (i.e. functional vessels) immediately filled with air (as observed by Torres-Ruiz et al. [2015]), whereas living vessels were not affected by cutting (i.e. cytoplasm was left intact in the individual vessel elements; Jacobsen et al., 2015). Filled vessels in these images were typically located in the outermost part of the xylem tissue and discarded in the subsequent analyses.

For each species and organ, the theoretical specific hydraulic conductivity of a whole cross section (K_H) was calculated from the Hagen-Poiseuille equation using the individual diameter of sap-filled and air-filled vessels as:

$$K_H = \sum \frac{\pi \cdot \emptyset^4}{128 \cdot \eta \cdot A_{Xyl}} \quad (1)$$

where K_H is the specific theoretical hydraulic conductivity (kg m^{-1} MPa^{-1} s^{-1}), Ø is the mean Feret diameter of vessels (m), η is the viscosity of water (1.002 mPa s^{-1} at 20°C), and A_{Xyl} is the xylem area of the cross section (m^2).

The theoretical loss of hydraulic conductivity (PLC) was calculated as:

$$PLC = 100 \cdot \frac{K_{HA}}{K_{HMax}} \quad (2)$$

with K_{HA} and K_{HMax} representing the theoretical hydraulic conductivities of air-filled vessels in initial and cut cross sections, respectively.

Vulnerability curves (PLC as a function of water potential) were fitted using the nls function of R software (R Development Core Team, 2013), according to the following equation:

$$PLC = \frac{1}{1 + e^{\frac{slp}{25}(\Psi - \Psi_{50})}} \quad (3)$$

with *slp* being the derivative at the inflection point Ψ_{50Stem}.

The air entry point (Ψ_e) was estimated from Equation 3 as $50/slp + \Psi_{50Stem}$ (Domec and Gartner, 2001).

K_{Leaf}

Loss of K_{Leaf} was measured using the rehydration kinetic method (Brodribb and Holbrook, 2003; Charra-Vaskou and Mayr, 2011) on eight *V. vinifera* 'Cabernet Sauvignon' plants (n = 4–5 measurements per plant). Conductance measurements were performed using plants at different levels of water stress. Two contiguous fully expanded leaves were bagged in plastic bags with wet paper towels for 1 h before taking a measurement in order to cease transpiration and equilibrate water potential within the leaf. Ψ_{Leaf} was measured on one leaf using a Scholander pressure chamber (Precis 2000), while K_{Leaf} was measured on the second one. The second leaf was excised and immediately connected, under water, to a flowmeter to measure K_{Leaf}. The flowmeter was composed of a pressure transducer (Omega Engineering) connected to a datalogger (USB-TC-AI; MCC), which measures the water pressure drop between a calibrated capillary PEEK tube and the leaf. This pressure drop was then converted into a flow rate to calculate the leaf conductance as the ratio between the maximum flow rate recorded during rehydration and the leaf water potential. Specific leaf conductance was calculated subsequently by dividing the leaf conductance by the leaf area, which was measured using a leaf area meter (WinFolia 2007b; Regent Instruments). The leaf vulnerability curve (percentage loss in K_{Leaf} as a function of water potential) was fitted using the nls function of R software (R Development Core Team, 2013), according to the equation:

$$PLK_{Leaf} = \frac{1}{1 + e^{\frac{slp}{25} \cdot (\Psi - \Psi_{50Leaf})}} \quad (4)$$

with *slp* being the derivative at the inflection point Ψ_{50Leaf}.

Gas Exchange

Predawn water potential (Ψ_{pd}) was measured on one leaf per plant, close to the rootstock prior to any light exposure, on nine *V. vinifera* 'Cabernet Sauvignon' plants exposed to different levels of water stress ($-0.05 < \Psi_{pd} < -2$ MPa). Plants were then exposed to outside ambient conditions from 8 AM until 2 PM during a sunny day (photosynthetically active radiation > 1,500 μmol m^{-2} s^{-1}; VPD > 2,000 Pa). Leaf gas-exchange measurements were conducted on mature, well-exposed leaves using a portable open system including an infrared gas analyzer (GFS 3000; Walz). Conditions in the cuvette (i.e. photosynthetically active radiation, temperature, VPD, and CO_2) were set equal to environmental conditions. Leaf transpiration rate (E; mmol m^{-2} s^{-1}) was measured during the morning, from 8 AM until 2 PM . Water potentials were measured on the leaf used for gas exchange (Ψ_{Leaf}) and on another one, wrapped for 1 h in a plastic bag covered with aluminum foil (Ψ_{Stem}), using a Scholander pressure chamber (Precis 2000). K_{Leaf_Ap} was calculated as the ratio between E and $\Delta\Psi = \Psi_{Stem} - \Psi_{Leaf}$:

$$K_{leaf_{Ap}} = \frac{E}{\Delta\Psi} \quad (5)$$

A leaf vulnerability curve (percentage loss in K_{Leaf_Ap} as a function of water potential) was fitted using the nls function of R software (R Development Core Team, 2013), according to the equation:

$$PLK_{Leaf\_Ap} = \frac{1}{1 + e^{\frac{slp}{25} \cdot \left(\Psi - \Psi_{50Leaf\_Ap}\right)}} \quad (6)$$

with *slp* being the derivative at the inflection point Ψ_{50Leaf_Ap}.

Fluorescein Diacetate Staining

Detection of the viability of x-ray-exposed xylem cells was performed using a 9.6-μm fluorescein diacetate (Sigma-Aldrich) solution, in combination with fluorescence light microscopy. One plant was analyzed 10 d after first exposure to x-rays. Stem slices were obtained from the exposed part and 10 cm above this area. The stem was cut transversely, into 5-mm-thick slices, and immediately submerged into fluorescein diacetate solution for 30 min in the dark. Samples were rinsed with deionized water and placed onto a microscope glass slide. The sample surface was excited with green fluorescent light (λ = 490 nm) generated by a SOLA light engine (SE 5-LCR-VB; Lumencor) and observed for light at $\lambda > 500$ nm for the detection of living and metabolically active tissue (green signal) using an Axiozoom V16 macroscope (Zeiss) connected to an Axiocam 105 camera (Zeiss).

Supplemental Data

The following supplemental materials are available.

Supplemental Figure S1. Cell vitality at a distal part of grapevine stems 10 d after x-ray exposure by HRCT scans.

Supplemental Figure S2. Recovery in water potential measured via different methods (i.e. stem psychrometer, pressure chamber and bagged leaf, and pressure transducer).

ACKNOWLEDGMENTS

We thank the PSICHE beamline (SOLEIL synchrotron facility), the TOMCAT beamline (Swiss Light Source, Paul Scherrer Institut), and the I12 beamline (Diamond Light Source); vitality imaging was performed at the Bordeaux Imaging Center, which is a member of the national infrastructure France BioImaging, with the help of Brigitte Batailler.

Received August 1, 2016; accepted September 8, 2016; published September 9, 2016.

LITERATURE CITED

Améglio T, Bodet C, Lacointe A, Cochard H (2002) Winter embolism, mechanisms of xylem hydraulic conductivity recovery and springtime growth patterns in walnut and peach trees. Tree Physiol **22:** 1211–1220

Améglio T, Decourteix M, Alves G, Valentin V, Sakr S, Julien JL, Petel G, Guilliot A, Lacointe A (2004) Temperature effects on xylem sap osmolarity in walnut trees: evidence for a vitalistic model of winter embolism repair. Tree Physiol **24:** 785–793

Améglio T, Ewers FW, Cochard H, Martignac M, Vandame M, Bodet C, Cruiziat P (2001) Winter stem xylem pressure in walnut trees: effects of carbohydrates, cooling and freezing. Tree Physiol **21:** 387–394

Bouche PS, Delzon S, Choat B, Badel E, Brodribb TJ, Burlett R, Cochard H, Charra-Vaskou K, Lavigne B, Li S, et al (2016) Are needles of *Pinus pinaster* more vulnerable to xylem embolism than branches? New insights from x-ray computed tomography. Plant Cell Environ **39:** 860–870

Brodersen CR, McElrone AJ, Choat B, Lee EF, Shackel KA, Matthews MA (2013) In vivo visualizations of drought-induced embolism spread in *Vitis vinifera*. Plant Physiol **161:** 1820–1829

Brodersen CR, McElrone AJ, Choat B, Matthews MA, Shackel KA (2010) The dynamics of embolism repair in xylem: in vivo visualizations using high-resolution computed tomography. Plant Physiol **154:** 1088–1095

Brodribb TJ, Holbrook NM (2003) Stomatal closure during leaf dehydration, correlation with other leaf physiological traits. Plant Physiol **132:** 2166–2173

Carbonneau A (1985) The early selection of grapevine rootstocks for resistance to drought conditions. Am J Enol Vitic **36:** 195–198

Charra-Vaskou K, Badel E, Burlett R, Cochard H, Delzon S, Mayr S (2012) Hydraulic efficiency and safety of vascular and non-vascular components in *Pinus pinaster* leaves. Tree Physiol **32:** 1161–1170

Charra-Vaskou K, Badel E, Charrier G, Ponomarenko A, Bonhomme M, Foucat L, Mayr S, Améglio T (2016) Cavitation and water fluxes driven by ice water potential in *Juglans regia* during freeze-thaw cycles. J Exp Bot **67:** 739–750

Charra-Vaskou K, Mayr S (2011) The hydraulic conductivity of the xylem in conifer needles (*Picea abies* and *Pinus mugo*). J Exp Bot **62:** 4383–4390

Charrier G, Charra-Vaskou K, Kasuga J, Cochard H, Mayr S, Améglio T (2014) Freeze-thaw stress: effects of temperature on hydraulic conductivity and ultrasonic activity in ten woody angiosperms. Plant Physiol **164:** 992–998

Charrier G, Cochard H, Améglio T (2013) Evaluation of the impact of frost resistances on potential altitudinal limit of trees. Tree Physiol **33:** 891–902

Charrier G, Ngao J, Saudreau M, Améglio T (2015) Effects of environmental factors and management practices on microclimate, winter physiology, and frost resistance in trees. Front Plant Sci **6:** 259

Choat B, Badel E, Burlett R, Delzon S, Cochard H, Jansen S (2016) Noninvasive measurement of vulnerability to drought-induced embolism by x-ray microtomography. Plant Physiol **170:** 273–282

Choat B, Drayton WM, Brodersen C, Matthews MA, Shackel KA, Wada H, McElrone AJ (2010) Measurement of vulnerability to water stress-induced cavitation in grapevine: a comparison of four techniques applied to a long-vesseled species. Plant Cell Environ **33:** 1502–1512

Choat B, Jansen S, Brodribb TJ, Cochard H, Delzon S, Bhaskar R, Bucci SJ, Feild TS, Gleason SM, Hacke UG, et al (2012) Global convergence in the vulnerability of forests to drought. Nature **491:** 752–755

Choat B, Lahr EC, Melcher PJ, Zwieniecki MA, Holbrook NM (2005) The spatial pattern of air seeding thresholds in mature sugar maple trees. Plant Cell Environ **28:** 1082–1089

Cobb AR, Choat B, Holbrook NM (2007) Dynamics of freeze-thaw embolism in *Smilax rotundifolia* (Smilacaceae). Am J Bot **94:** 640–649

Cochard H, Badel E, Herbette S, Delzon S, Choat B, Jansen S (2013) Methods for measuring plant vulnerability to cavitation: a critical review. J Exp Bot **64:** 4779–4791

Cochard H, Coll L, Le Roux X, Améglio T (2002) Unraveling the effects of plant hydraulics on stomatal closure during water stress in walnut. Plant Physiol **128:** 282–290

Cochard H, Delzon S (2013) Hydraulic failure and repair are not routine in trees. Ann For Sci **70:** 659–661

Cochard H, Delzon S, Badel E (2015) X-ray microtomography (micro-CT): a reference technology for high-resolution quantification of xylem embolism in trees. Plant Cell Environ **38:** 201–206

Cochard H, Lemoine D, Améglio T, Granier A (2001) Mechanisms of xylem recovery from winter embolism in Fagus sylvatica. Tree Physiol **21:** 27–33

Dalla-Salda G, Fernández ME, Sergent AS, Rozenberg P, Badel E, Martinez-Meier A (2014) Dynamics of cavitation in a Douglas-fir tree-ring: transition-wood, the lord of the ring? Journal of Plant Hydraulics **1:** e-0005

Dixon HH (1896) Transpiration into a saturated atmosphere. Proceedings of the Royal Irish Academy (1889–1901) **4:** 627–635

Domec JC, Gartner BL (2001) Cavitation and water storage capacity in bole xylem segments of mature and young Douglas-fir trees. Trees (Berl) **15:** 204–214

Ennajeh M, Simões F, Khemira H, Cochard H (2011) How reliable is the double-ended pressure sleeve technique for assessing xylem vulnerability to cavitation in woody angiosperms? Physiol Plant **142:** 205–210

Ewers FW, Améglio T, Cochard H, Beaujard F, Martignac M, Vandame M, Bodet C, Cruiziat P (2001) Seasonal variation in xylem pressure of walnut trees: root and stem pressures. Tree Physiol **21:** 1123–1132

Ewers FW, Cochard H, Tyree MT (1997) A survey of root pressures in vines of a tropical lowland forest. Oecologia **110:** 191–196

Hacke UG, Sauter JJ (1996) Xylem dysfunction during winter and recovery of hydraulic conductivity in diffuse-porous and ring-porous trees. Oecologia **105:** 435–439

Hacke UG, Sperry JS (2003) Limits to xylem refilling under negative pressure in *Laurus nobilis* and *Acer negundo*. Plant Cell Environ **26:** 303–311

Hacke UG, Venturas MD, MacKinnon ED, Jacobsen AL, Sperry JS, Pratt RB (2015) The standard centrifuge method accurately measures vulnerability curves of long-vesselled olive stems. New Phytol **205:** 116–127

Hales S (1727) Vegetable Staticks, or an Account of Some Statical Experiments on the Sap in Vegetables. J Peele, London

Hartmann H (2015) Carbon starvation during drought-induced tree mortality: are we chasing a myth? Journal of Plant Hydraulics **2:** e005

Hartmann H, Ziegler W, Kolle O, Trumbore S (2013) Thirst beats hunger: declining hydration during drought prevents carbon starvation in Norway spruce saplings. New Phytol **200:** 340–349

Hochberg U, Albuquerque C, Rachmilevitch S, Cochard H, David-Schwartz R, Brodersen CR, McElrone A, Windt CW (2016) Grapevine petioles are more sensitive to drought induced embolism than stems: evidence from in vivo MRI and microCT observations of hydraulic vulnerability segmentation. Plant Cell Environ **39:** 1886–1894

Holbrook NM, Ahrens ET, Burns MJ, Zwieniecki MA (2001) In vivo observation of cavitation and embolism repair using magnetic resonance imaging. Plant Physiol **126:** 27–31

Holbrook NM, Zwieniecki MA (1999) Embolism repair and xylem tension: do we need a miracle? Plant Physiol **120:** 7–10

Jacobsen AL, Pratt RB (2012) No evidence for an open vessel effect in centrifuge-based vulnerability curves of a long-vesselled liana (*Vitis vinifera*). New Phytol **194:** 982–990

Jacobsen AL, Rodriguez-Zaccaro FD, Lee TF, Valdovinos J, Toschi HS, Martinez JA, Pratt RB (2015) Grapevine xylem development, architecture and function. *In* Functional and Ecological Xylem Anatomy. Springer International Publishing, Berlin, Germany pp 133–162

Jansen S, Choat B, Pletsers A (2009) Morphological variation of intervessel pit membranes and implications to xylem function in angiosperms. Am J Bot **96:** 409–419

Jones HG, Sutherland RA (1991) Stomatal control of xylem embolism. Plant Cell Environ **14:** 607–612

Kim YX, Steudle E (2007) Light and turgor affect the water permeability (aquaporins) of parenchyma cells in the midrib of leaves of *Zea mays*. J Exp Bot **58:** 4119–4129

Knipfer T, Cuneo IF, Brodersen CR, McElrone AJ (2016) In situ visualization of the dynamics in xylem embolism formation and removal in the absence of root pressure: a study on excised grapevine stems. Plant Physiol **171:** 1024–1036

Knipfer T, Eustis A, Brodersen C, Walker AM, McElrone AJ (2015) Grapevine species from varied native habitats exhibit differences in embolism formation/repair associated with leaf gas exchange and root pressure. Plant Cell Environ **38:** 1503–1513

Lens F, Sperry JS, Christman MA, Choat B, Rabaey D, Jansen S (2011) Testing hypotheses that link wood anatomy to cavitation resistance and hydraulic conductivity in the genus *Acer*. New Phytol **190:** 709–723

Lovisolo C, Perrone I, Carra A, Ferrandino A, Flexas J, Medrano H, Schubert A (2010) Drought-induced changes in development and function of grapevine (*Vitis* spp.) organs and in their hydraulic and non-hydraulic interactions at the whole-plant level: a physiological and molecular update. Funct Plant Biol **37:** 98–116

Maherali H, Pockman WT, Jackson RB (2004) Adaptive variation in the vulnerability of woody plants to xylem cavitation. Ecology **85:** 2184–2199

Martin-StPaul NK, Longepierre D, Huc R, Delzon S, Burlett R, Joffre R, Rambal S, Cochard H (2014) How reliable are methods to assess xylem vulnerability to cavitation? The issue of 'open vessel' artifact in oaks. Tree Physiol **34:** 894–905

McDowell NG (2011) Mechanisms linking drought, hydraulics, carbon metabolism, and vegetation mortality. Plant Physiol **155:** 1051–1059

Mencuccini M (2003) The ecological significance of long-distance water transport: short-term regulation, long-term acclimation and the hydraulic costs of stature across plant life forms. Plant Cell Environ **26:** 163–182

Mirone A, Brun E, Gouillart E, Tafforeau P, Kieffer J (2014) The PyHST2 hybrid distributed code for high speed tomographic reconstruction with iterative reconstruction and a priori knowledge capabilities. Nucl Instrum Methods Phys Res B **324:** 41–48

Nardini A, Lo Gullo MA, Salleo S (2011) Refilling embolized xylem conduits: is it a matter of phloem unloading? Plant Sci **180:** 604–611

Nardini A, Salleo S (2000) Limitation of stomatal conductance by hydraulic traits: sensing or preventing xylem cavitation? Trees (Berl) **15:** 14–24

Nolf M, Creek D, Duursma R, Holtum J, Mayr S, Choat B (2015) Stem and leaf hydraulic properties are finely coordinated in three tropical rain forest tree species. Plant Cell Environ **38:** 2652–2661

Ogasa MY, Utsumi Y, Miki NH, Yazaki K, Fukuda K (2016) Cutting stems before relaxing xylem tension induces artefacts in *Vitis coignetiae*, as evidenced by magnetic resonance imaging. Plant Cell Environ **39:** 329–337

Paganin D, Mayo SC, Gureyev TE, Miller PR, Wilkins SW (2002) Simultaneous phase and amplitude extraction from a single defocused image of a homogeneous object. J Microsc **206:** 33–40

Ponomarenko A, Vincent O, Pietriga A, Cochard H, Badel É, Marmottant P (2014) Ultrasonic emissions reveal individual cavitation bubbles in water-stressed wood. J R Soc Interface **11:** 20140480

Pratt RB, MacKinnon ED, Venturas MD, Crous CJ, Jacobsen AL (2015) Root resistance to cavitation is accurately measured using a centrifuge technique. Tree Physiol **35:** 185–196

R Development Core Team (2013) R: A Language and Environment for Statistical Computing. R Foundation for Statistical Computing, Vienna, https://www.R-project.org

Rockwell FE, Wheeler JK, Holbrook NM (2014) Cavitation and its discontents: opportunities for resolving current controversies. Plant Physiol **164:** 1649–1660

Rood SB, Patiño S, Coombs K, Tyree MT (2000) Branch sacrifice: cavitation-associated drought adaptation of riparian cottonwoods. Trees (Berl) **14:** 248–257

Sala A, Woodruff DR, Meinzer FC (2012) Carbon dynamics in trees: feast or famine? Tree Physiol **32:** 764–775

Salleo S, Gullo MAL, Paoli D, Zippo M (1996) Xylem recovery from cavitation-induced embolism in young plants of Laurus nobilis: a possible mechanism. New Phytol **132:** 47–56

Schenk HJ, Steppe K, Jansen S (2015) Nanobubbles: a new paradigm for air-seeding in xylem. Trends Plant Sci **20:** 199–205

Schultz HR (2003) Differences in hydraulic architecture account for near-isohydric and anisohydric behaviour of two field-grown *Vitis vinifera* L. cultivars during drought. Plant Cell Environ **26:** 1393–1405

Scoffoni C, Vuong C, Diep S, Cochard H, Sack L (2014) Leaf shrinkage with dehydration: coordination with hydraulic vulnerability and drought tolerance. Plant Physiol **164:** 1772–1788

Sperry J (2013) Cutting-edge research or cutting-edge artefact? An overdue control experiment complicates the xylem refilling story. Plant Cell Environ **36:** 1916–1918

Sperry JS (1988) Winter xylem embolism and spring recovery in Betula cordifolia, Fagus grandifolia, Abies balsamea and Picea rubens. *In* M Borghetti, J Grace, A Raschi, eds, Water Transport in Plants under Climatic Stress. Cambridge University Press, Cambridge, UK, pp 86–98

Sperry JS, Christman MA, Torres-Ruiz JM, Taneda H, Smith DD (2012) Vulnerability curves by centrifugation: is there an open vessel artefact, and are 'r' shaped curves necessarily invalid? Plant Cell Environ **35:** 601–610

Sperry JS, Holbrook NM, Zimmermann MH, Tyree MT (1987) Spring filling of xylem vessels in wild grapevine. Plant Physiol **83:** 414–417

Sperry JS, Nichols KL, Sullivan JE, Eastlack SE (1994) Xylem embolism in ring-porous, diffuse-porous, and coniferous trees of northern Utah and interior Alaska. Ecology **75:** 1736–1752

Thitithanakul S, Pétel G, Chalot M, Beaujard F (2012) Supplying nitrate before bud break induces pronounced changes in nitrogen nutrition and growth of young poplars. Funct Plant Biol **39:** 795–803

Tombesi S, Nardini A, Farinelli D, Palliotti A (2014) Relationships between stomatal behavior, xylem vulnerability to cavitation and leaf water relations in two cultivars of *Vitis vinifera*. Physiol Plant **152:** 453–464

Torres-Ruiz JM, Cochard H, Mayr S, Beikircher B, Diaz-Espejo A, Rodriguez-Dominguez CM, Badel E, Fernández JE (2014) Vulnerability to cavitation in Olea europaea current-year shoots: further evidence of an open-vessel artifact associated with centrifuge and air-injection techniques. Physiol Plant **152:** 465–474

Torres-Ruiz JM, Jansen S, Choat B, McElrone AJ, Cochard H, Brodribb TJ, Badel E, Burlett R, Bouche PS, Brodersen CR, et al (2015) Direct x-ray microtomography observation confirms the induction of embolism upon xylem cutting under tension. Plant Physiol **167:** 40–43

Tyree MT, Salleo S, Nardini A, Mosca R, Assunta Lo Gullo M, Mosca R (1999) Refilling of embolized vessels in young stems of laurel: do we need a new paradigm? Plant Physiol **120:** 11–22

Tyree MT, Sperry JS (1988) Do woody plants operate near the point of catastrophic xylem dysfunction caused by dynamic water stress? Answers from a model. Plant Physiol **88:** 574–580

Tyree MT, Zimmermann MH (2002) Xylem Structure and the Ascent of Sap. Springer-Verlag, Berlin

Umebayashi T, Ogasa MY, Miki NH, Utsumi Y, Haishi T, Fukuda K (2016) Freezing xylem conduits with liquid nitrogen creates artifactual embolisms in water-stressed broadleaf trees. Trees (Berl) **30:** 305–316

Vergeynst LL, Dierick M, Bogaerts JA, Cnudde V, Steppe K (2015) Cavitation: a blessing in disguise? New method to establish vulnerability curves and assess hydraulic capacitance of woody tissues. Tree Physiol **35:** 400–409

Wheeler JK, Huggett BA, Tofte AN, Rockwell FE, Holbrook NM (2013) Cutting xylem under tension or supersaturated with gas can generate PLC and the appearance of rapid recovery from embolism. Plant Cell Environ **36:** 1938–1949

Wheeler JK, Sperry JS, Hacke UG, Hoang N (2005) Inter-vessel pitting and cavitation in woody Rosaceae and other vesselled plants: a basis for a safety versus efficiency trade-off in xylem transport. Plant Cell Environ **28:** 800–812

Zecca G, Abbott JR, Sun WB, Spada A, Sala F, Grassi F (2012) The timing and the mode of evolution of wild grapes (*Vitis*). Mol Phylogenet Evol **62:** 736–747

Zhang YJ, Holbrook NM (2014) The stability of xylem water under tension: a long, slow spin proves illuminating. Plant Cell Environ **37:** 2652–2653

Zufferey V, Cochard H, Ameglio T, Spring JL, Viret O (2011) Diurnal cycles of embolism formation and repair in petioles of grapevine (*Vitis vinifera* cv. Chasselas). J Exp Bot **62:** 3885–3894

Zwieniecki MA, Holbrook NM (2000) Bordered pit structure and vessel wall surface properties: implications for embolism repair. Plant Physiol **123:** 1015–1020